PERGAMON

International Journal of Solids and Structures 40 (2003) 6111–6123

INTERNATIONAL JOURNAL OF SOLIDS and STRUCTURES

www.elsevier.com/locate/ijsolstr

Analysis of thin-walled curved box beam under in-plane flexure

Youngkyu Kim, Yoon Young Kim *

School of Mechanical and Aerospace Engineering, National Creative Research Initiatives Center for Multiscale Design, Seoul National University, San 56-1, Shinlim-Dong, Kwanak-Gu, Seoul 151-744, South Korea

Received 16 October 2002

Abstract

A higher-order one-dimensional analysis of the in-plane flexural deformation of thin-walled curved box beams is carried out. The main contribution of the present work is to consider an additional degree of freedom accounting for the in-plane distortional deformation of the thin-walled cross section that is accompanied by the in-plane bending deformation. Especially, we develop a systematic procedure to determine this bending distortion and formulate a higher-order beam theory including this additional degree of freedom. The significant contribution of the bending distortion to the beam flexibility is clearly demonstrated through several case studies.

Keywords: Thin-walled beam; Curved beam; Bending distortion; Box beam; Cross section; Finite element method

1. Introduction

A comprehensive analysis of thin-walled open and closed beams was carried out by Vlasov (1961), and extended by Dabrowski (1968) for the analysis of thin-walled curved girders. Vlasov's theory is also used to develop a thin-walled beam element by Fu and Hsu (1995). Recently, Kim and Kim (1999a,b, 2000) have developed a higher-order one-dimensional theory for thin-walled closed straight beams under torsion, torsional distortion, and torsional warping. These investigations have addressed the significant effects of distortion and warping deformations on the analysis accuracy. (For more references on this subject, see the references cited in Kim and Kim, 2000 and Kim et al., 2002.) Paulsen and Welo (2001) have also shown the effect of the hour-glass section distortion on the buckling phenomena of hollow rectangular beams.

To consider the effect of curvature on the flexibility and stress concentration of thin-walled structures, Whatham (1986) studied the bending characteristics of a thin-walled curved pipe system using a thin-shell theory, and Lewis and Chao (1990) derived the flexibility factors of trunnion piping elbows. In the case of thin-walled circular cross sections, the ovalization of cross sections (Beskin, 1945) is known to increase the flexibility of pipe systems. Hu and Li (1999) also studied elastic–plastic bending problems of pipes. These

* Corresponding author. Tel.: +82-2-880-7154; fax: +82-2-883-1513.
E-mail addresses: youngkyu@idealab.snu.ac.kr (Y. Kim), yykim@snu.ac.kr (Y.Y. Kim).

0020-7683/$ - see front matter © 2003 Elsevier Ltd. All rights reserved.
doi:10.1016/S0020-7683(03)00367-6

efforts were successful in predicting the additional flexibility of thin-walled curved elbows, but limited to circular sections only.

Although thin-walled curved beams having arbitrary cross sections are used in many engineering applications, such as automobile bodies and high way bridges, there appears no one-dimensional theory yielding satisfactory results for thin-walled closed curved beams. Since the well-known Timoshenko beam theory does not give accurate results for thin-walled curved box beams, we aim at developing a one-dimensional higher-order beam theory for such beams. Though higher-order theories are available, they are applicable only to solid curved beams or to thin-walled straight beams. For accurate in-plane flexural analysis of thin-walled curved box beams, we propose to include an additional degree of freedom representing the symmetric sectional deformation mode in addition to the three degrees of freedom typically employed in the Timoshenko theory.

The main contribution of the present work is to find an approximate shape for the symmetric sectional deformation and to derive the higher-order one-dimensional theory for the in-plane flexural analysis of the thin-walled curved box beam. In the case of a rectangular hollow cross section, out-of-plane flexural and torsional deformations are decoupled with in-plane flexural deformation. Since the one-dimensional analysis of the out-of-plane flexural deformation has already been worked out by the present authors (Kim and Kim, 2002), the present work is mainly focused on the in-plane flexural analysis of thin-walled curved box beams.

2. Bending distortion

Fig. 1 shows a thin-walled curved box beam with its geometric dimensions. The global coordinate system (ρ, ϕ, y) is also shown in Fig. 1. To address the need to develop a higher-order one-dimensional theory for accurate analysis, we may consider a cantilevered thin-walled curved box beam shown in Fig. 2. One end is fixed and the other end, rigidly constrained so that the cross section at the end always remains undeformed. The external forces acting at the end of the beam may be decomposed into a tangential force T, a radial force V and an in-plane bending moment M. The three displacement components in the direction of T, V, and M are the tangential displacement u, the radial displacement v, and the rotation angle β.

Before presenting the present development of a higher-order theory, we begin with checking the accuracy of the Timoshenko beam theory employing the three displacement components based on the Timoshenko kinematics for the thin-walled curved box beams. In Fig. 3, the radial displacement $v(\phi)$ along the center line C of the cantilever beam under the tip bending moment $M = 1$ Nm. The beam geometry and the

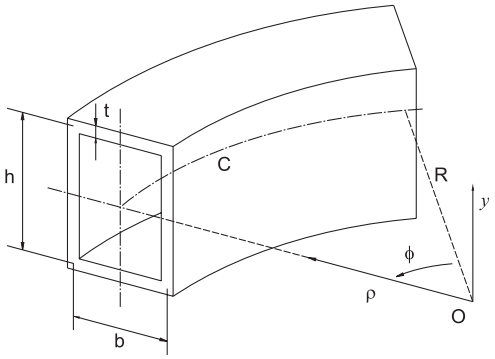

Fig. 1. The geometry and coordinate system of a thin-walled curved beam having a rectangular cross section.

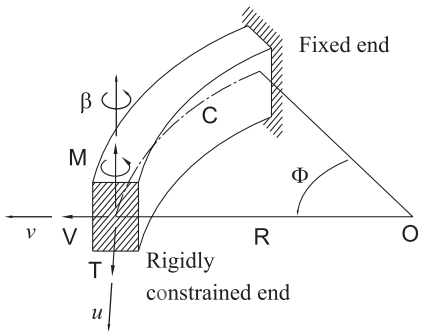

Fig. 2. A cantilevered thin-walled curved box beam subjected to external loads and corresponding displacement components.

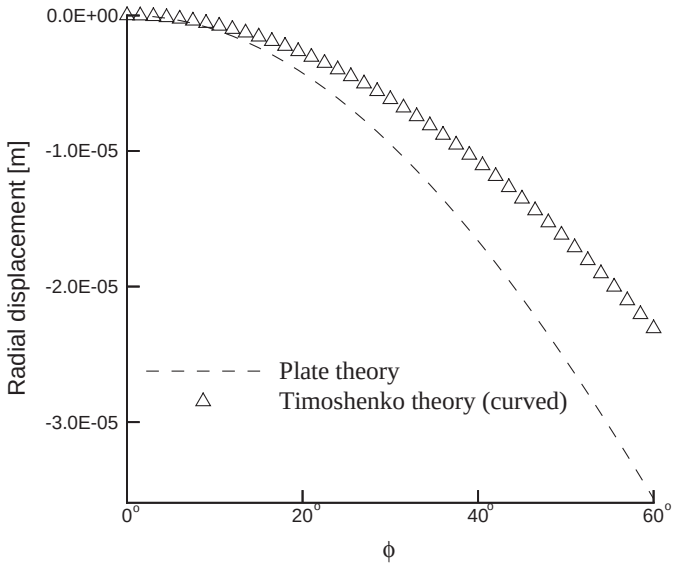

Fig. 3. The radial displacement $v(\phi)$ of the centerline of the beam shown in Fig. 2 as a function of ϕ ($b = 50$ mm, $h = 70$ mm, $t = 1$ mm, $R = 1$ m, $E = 200$ GPa, $v = 0.3$, $\Phi = 60°$, $M = 1$ Nm).

material property are given in Fig. 3. From Fig. 3, it is clear that the one-dimensional result by the Timoshenko theory gives quite inaccurate results in comparison with the plate finite element result (I-DEAS, 1993). The inaccuracy of the Timoshenko theory arises from the fact that the Timoshenko theory does not consider in-plane cross section deformations. Unlike in solid beams, in-plane cross section deformations are not negligible in thin-walled box beams. Therefore, a higher-order beam theory needs to be developed to predict accurately the behavior of thin-walled curved box beams.

In finding in-plane sectional deformation shape functions of thin-walled curved box beams, one may consider the fundamental section deformation modes illustrated in Fig. 4. Vlasov (1961) noted that the torsional distortion mode shown in Fig. 4(b) is accompanied by torsion. Kim and Kim (1999a,b, 2000) have incorporated this torsional distortion mode to analyze the coupled deformations of torsion, torsional distortion, and torsional warping in thin-walled beams with rectangular or quadrilateral cross sections. The present authors (2002) have also adopted this torsional distortion mode for the accurate prediction of the deflection of the thin-walled curved box beams under out-of-plane bending coupled with torsion.

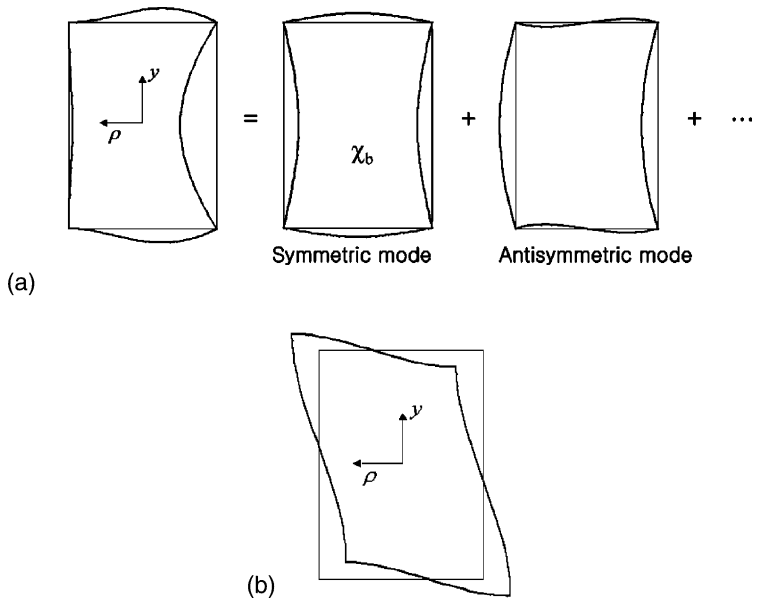

Fig. 4. In-plane cross section deformation modes of the thin-walled curved box beam: (a) deformation mode accompanied by the bending moment about y-axis and (b) torsional distortion mode (thin: undeformed, bold: deformed).

The deformation shape shown in Fig. 4(a) may be accompanied by the in-plane flexural bending deformation of a thin-walled curved box beam when it is subjected to a bending moment about the y-axis. Due to the curvature effect, the accompanied deformation may be not symmetric with respect to the y-axis. This cross section deformation affects significantly the flexibility of a thin-walled curved box beam, and can be decomposed into the symmetric and antisymmetric modes and the higher modes. From the present authors' unpublished investigation, it can be concluded that the additional flexibility due to the cross section deformation is mainly due to the symmetric mode shown in Fig. 4(a), as far as the radius of curvature is not so small. For more accurate analysis of the thin-walled curved box beam with a small radius of curvature, one may need to take into account the antisymmetric mode (and higher modes). The goal of the present work, however, is to derive the one-dimensional theory for the in-plane flexure of a thin-walled curved box beam that is as simple as possible; therefore we select only one degree of freedom representing the symmetric mode, which will be called the bending distortion χ_b throughout this work.

To determine the explicit formula representing the deformation shape of bending distortion χ_b, it may be convenient to treat four walls of a rectangular box beam separately as shown in Fig. 5. Fig. 5 also shows the local coordinate systems (n_i, s_i, ϕ) (where $i = 1, 2, 3, 4$) attached to each of four walls, which will be used to facilitate subsequent analysis.

The displacement components along the contour line of the beam cross section due to bending distortion χ_b may be written as

$$u_{ni}(s_i, \phi) = \psi_{ni}^{\chi_b}(s_i)\chi_b(\phi) \tag{1a}$$

$$u_{si}(s_i, \phi) = \psi_{si}^{\chi_b}(s_i)\chi_b(\phi) \tag{1b}$$

$$u_{\phi i}(s_i, \phi) = \psi_{\phi i}^{\chi_b}(s_i)\chi_b(\phi) \tag{1c}$$

where ψ's represent the shape functions of each piece of the beam cross section which must be determined. The quantities associated with the ith wall are designated by subscript i.

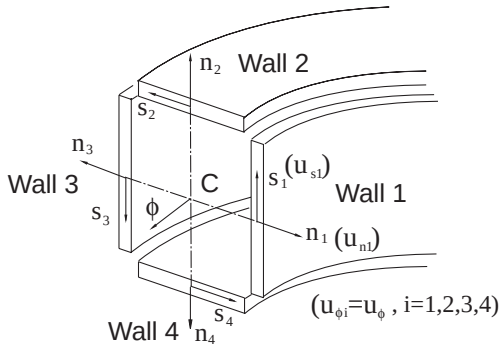

Fig. 5. Local coordinates for each wall of a thin-walled curved rectangular box beam.

Considering the fact that the bending distortion χ_b is dominated by the in-plane bending of walls and neglecting the unloading effect or shear lag (Krístek, 1979), one may assume that

$$\psi_{si}^{\chi_b}(s_i) = \psi_{\phi i}^{\chi_b}(s_i) = 0, \qquad \psi_{ni}^{\chi_b}(s_i) \neq 0$$

Since a complicated analysis to determine the shape function $\psi_{ni}^{\chi_b}$ for the bending distortion χ_b does not merit one-dimensional beam analysis, we will derive an approximate shape function by using a quarter model of the cross section shown in Fig. 6(a). Because both the geometry and external loads due to the in-plane flexure are symmetric with respect to the two symmetry axes of the hollow rectangular cross section, the shape function $\psi_{ni}^{\chi_b}$ of the bending distortion may be assumed to be symmetric. Based on this observation, the deformed shape of the quarter model is depicted in Fig. 6(b).

The apparent bending deformation of the walls in Fig. 6(b) in the ρ–y plane may be well approximated by the Euler–Bernoulli beam theory ($b, h \gg t$). Thus, the outward normal displacements $\psi_{ni}^{\chi_b}$ of the contour line of the beam cross section may be written as homogeneous solutions of the Euler–Bernoulli beam equations:

$$\psi_{n1}^{\chi_b}(s_1) = a_0 + a_1 s_1 + a_2 s_1^2 + a_3 s_1^3 \quad \left(0 \leqslant s_1 \leqslant \frac{h}{2}\right) \tag{2a}$$

$$\psi_{n2}^{\chi_b}(s_2) = b_0 + b_1 s_2 + b_2 s_2^2 + b_3 s_2^3 \quad \left(-\frac{b}{2} \leqslant s_2 \leqslant 0\right) \tag{2b}$$

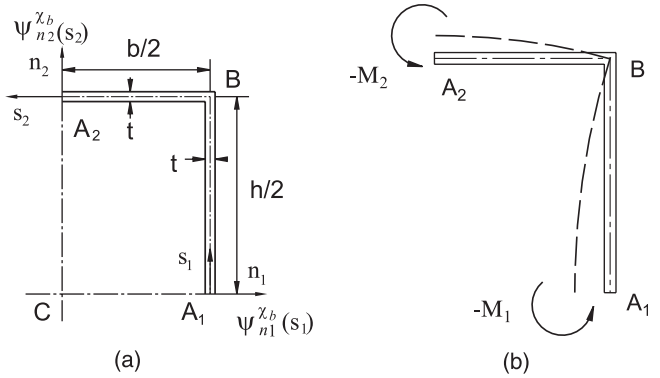

Fig. 6. (a) Local coordinate systems of a quarter model of the rectangular cross section (A_1 and A_2 are the middle points of walls 1 and 2, respectively) and (b) internal moments acting at wall 1 and 2 and the wall deformation.

The outward displacements for $\left(-\frac{h}{2} \leqslant s_1 \leqslant 0\right)$ and $\left(0 \leqslant s_2 \leqslant \frac{b}{2}\right)$ can be obtained by changing the signs of (a_1, a_3, b_1, b_3).

To determine the coefficients a_j, b_j $(j = 0, 1, 2, 3)$, the following conditions are used. First, each wall is assumed to be inextensional so that the normal displacements at corner B vanish:

$$\psi_{n1}^{\chi_b}\left(s_1 = \frac{h}{2}\right) = \psi_{n2}^{\chi_b}\left(s_2 = -\frac{b}{2}\right) = 0 \tag{3}$$

Second, the slopes of the normal displacements at $s_1 = s_2 = 0$ must vanish from the symmetry condition (see Fig. 4(a)):

$$\frac{\mathrm{d}\psi_{n1}^{\chi_b}}{\mathrm{d}s_1}(s_1 = 0) = \frac{\mathrm{d}\psi_{n2}^{\chi_b}}{\mathrm{d}s_2}(s_2 = 0) = 0 \tag{4}$$

The slope continuity condition and the moment equilibrium condition at corner B must be satisfied:

$$\frac{\mathrm{d}\psi_{n1}^{\chi_b}}{\mathrm{d}s_1}\left(s_1 = \frac{h}{2}\right) = \frac{\mathrm{d}\psi_{n2}^{\chi_b}}{\mathrm{d}s_2}\left(s_2 = -\frac{b}{2}\right) \tag{5}$$

$$\sum_{j=1}^{2} M_j = M_1\left(s_1 = \frac{h}{2}\right) + \left(-M_2\left(s_2 = -\frac{b}{2}\right)\right) = 0 \tag{6}$$

where each wall of the cross section is assumed to be in the condition of plane stress. Thus the bending moment–curvature relation may be given by

$$M_i(s_i) = \frac{Et^3}{12(1-\nu^2)}\frac{\mathrm{d}^2\psi_{ni}^{\chi_b}}{\mathrm{d}s_i^2}$$

The final condition to consider is the antisymmetry of deformations around corner B. To obtain the deformation shown in Fig. 6(b), we observe that the bending moments in the two adjacent walls around B must satisfy the following conditions:

$$M_1\left(s_1 = \frac{h}{2}\right) \geqslant 0, \qquad M_2\left(s_2 = -\frac{b}{2}\right) \leqslant 0 \tag{7}$$

Combining Eqs. (6) and (7) yields the vanishing moment condition at the corner as

$$M_1\left(s_1 = \frac{h}{2}\right) = M_2\left(s_2 = -\frac{b}{2}\right) = 0$$

Equivalently,

$$\frac{\mathrm{d}^2\psi_{n1}^{\chi_b}}{\mathrm{d}s_1^2}\left(s_1 = \frac{h}{2}\right) = \frac{\mathrm{d}^2\psi_{n2}^{\chi_b}}{\mathrm{d}s_2^2}\left(s_2 = -\frac{b}{2}\right) = 0 \tag{8}$$

Using seven conditions stated by Eqs. (3)–(5), and (8), the shape functions $\psi_{n1}^{\chi_b}(s_1)$ and $\psi_{n2}^{\chi_b}(s_2)$ of Eq. (2) can be determined as

$$\psi_{n1}^{\chi_b}(s_1) = \begin{cases} -\frac{h}{3} + \frac{2}{h}s_1^2 + \frac{4}{3h^2}s_1^3 & \left(-\frac{h}{2} \leqslant s_1 \leqslant 0\right) \\ -\frac{h}{3} + \frac{2}{h}s_1^2 - \frac{4}{3h^2}s_1^3 & \left(0 \leqslant s_1 \leqslant \frac{h}{2}\right) \end{cases}$$
$$\psi_{n2}^{\chi_b}(s_2) = \begin{cases} \frac{b}{3} - \frac{2}{b}s_2^2 - \frac{4}{3b^2}s_2^3 & \left(-\frac{b}{2} \leqslant s_2 \leqslant 0\right) \\ \frac{b}{3} - \frac{2}{b}s_2^2 + \frac{4}{3b^2}s_2^3 & \left(0 \leqslant s_2 \leqslant \frac{b}{2}\right) \end{cases} \tag{9}$$

Due to the symmetry, $\psi_{n3}^{\chi_b}(s_3)$ and $\psi_{n4}^{\chi_b}(s_4)$ are simply

$$\psi_{n3}^{\chi_b}(s_3) = \psi_{n1}^{\chi_b}(s_1)$$

$$\psi_{n4}^{\chi_b}(s_4) = \psi_{n2}^{\chi_b}(s_2)$$

3. One-dimensional field equation

In this section, we derive higher-order one-dimensional field equations considering the usual kinematic variables (u, v, ϕ) as well as the bending distortion variable χ_b. Here, we follow the procedure used for the analysis of thin-walled straight closed beams (Kim and Kim, 2000). First, the shell displacements of the contour line can be written as

$$u_{ni}(s_i, \phi) = \psi_{ni}^{v}(s_i)v(\phi) + \psi_{ni}^{\chi_b}(s_i)\chi_b(\phi) \tag{10a}$$

$$u_{si}(s_i, \phi) = \psi_{si}^{v}(s_i)v(\phi) \tag{10b}$$

$$u_{\phi i}(s_i, \phi) = \psi_{\phi i}^{u}(s_i)u(\phi) + \psi_{\phi i}^{\beta}(s_i)\beta(\phi) \tag{10c}$$

where only nonvanishing components of the deformation shape functions $\psi(s_i)$'s are kept.

For completeness, the Timoshenko kinematics is written as

$$\psi_{\phi i}^{u}(s_i) = 1 \quad (i = 1, 2, 3, 4)$$
$$\psi_{ni}^{v}(s_i) = \begin{cases} (-1)^{(i+1)/2} & (i = 1, 3) \\ 0 & (i = 2, 4) \end{cases}$$
$$\psi_{si}^{v}(s_i) = \begin{cases} 0 & (i = 1, 3) \\ (-1)^{(i-2)/2} & (i = 2, 4) \end{cases} \tag{11}$$
$$\psi_{\phi i}^{\beta}(s_i) = \begin{cases} (-1)^{(i+1)/2}\frac{b}{2} & (i = 1, 3) \\ (-1)^{(i-2)/2}s_i & (i = 2, 4) \end{cases}$$

Using the shell displacements of the contour, the three-dimensional displacements $\tilde{\boldsymbol{u}}_{ni}$, $\tilde{\boldsymbol{u}}_{si}$, and $\tilde{\boldsymbol{u}}_{\phi i}$ of a generic point in the beam cross section can be expressed as

$$\tilde{\boldsymbol{u}}_{ni}(n_i, s_i, \phi) \approx u_{ni}(s_i, \phi) = \psi_{ni}^{v}(s_i)u(\phi) + \psi_{ni}^{\chi_b}(s_i)\chi_b(\phi)$$

$$\tilde{\boldsymbol{u}}_{si}(n_i, s_i, \phi) \approx u_{si}(s_i, \phi) - n_i\frac{\partial u_{ni}^{\chi_b}(s_i, \phi)}{\partial s_i} = \psi_{si}^{v}(s_i)v(\phi) - n_i\frac{\mathrm{d}\psi_{ni}^{\chi_b}(s_i)}{\mathrm{d}s_i}\chi_b(\phi)$$

$$\tilde{\boldsymbol{u}}_{\phi i}(n_i, s_i, \phi) \approx u_{\phi i}(s_i, \phi) = \psi_{\phi i}^{u}(s_i)u(\phi) + \psi_{\phi i}^{\beta}(s_i)\beta(\phi)$$

The three-dimensional strain field then becomes

$$\epsilon_{zzi}(n_i,s_i,z)=\left\{\xi_i^2\left(1+\xi_i\frac{b}{2R}\right)+\zeta_i^2\left(1+\zeta_i\frac{s_i}{R}\right)\right\}\psi_{zi}^{u}(s)\frac{\mathrm{d}u(z)}{\mathrm{d}z}+\left\{-\frac{\xi_i}{R}\left(1+\xi_i\frac{b}{2R}\right)\psi_{ni}^{v}(s)-\frac{\zeta_i}{R}\left(1+\zeta_i\frac{s_i}{R}\right)\psi_{si}^{v}(s)\right\}v(z)+\left\{\xi_i^2\left(1+\xi_i\frac{b}{2R}\right)+\zeta_i^2\left(1+\zeta_i\frac{s_i}{R}\right)\right\}\psi_{zi}^{\beta}(s_i)\frac{\mathrm{d}\beta(z)}{\mathrm{d}z}+\left\{-\frac{\xi_i}{R}\left(1+\xi_i\frac{b}{2R}\right)\psi_{ni}^{\chi_\mathrm{b}}(s)+\frac{\zeta_i}{R}\left(1+\zeta_i\frac{s_i}{R}\right)n_i\frac{\mathrm{d}\psi_{ni}^{\chi_\mathrm{b}}(s)}{\mathrm{d}s_i}\right\}\chi_\mathrm{b}(z) \tag{12a}$$

$$\epsilon_{szi}(n_i,s_i,z)=\frac{1}{2}\left[\frac{\zeta_i}{R}\left(1+\zeta_i\frac{s_i}{R}\right)\psi_{zi}^{u}(s)u(z)+\zeta_i^2\left(1+\zeta_i\frac{s_i}{R}\right)\psi_{si}^{v}(s_i)\frac{\mathrm{d}v(z)}{\mathrm{d}z}+\left\{\zeta_i^2\frac{\mathrm{d}\psi_{zi}^{\beta}(s_i)}{\mathrm{d}s}+\frac{\zeta_i}{R}\left(1+\zeta_i\frac{s_i}{R}\right)\psi_{zi}^{\beta}(s_i)\right\}\beta(z)+\left\{-\xi_i^2\left(1+\xi_i\frac{b}{2R}\right)-\zeta_i^2\left(1+\zeta_i\frac{s_i}{R}\right)\right\}n_i\frac{\mathrm{d}\psi_{ni}^{\chi_\mathrm{b}}(s)}{\mathrm{d}s_i}\frac{\mathrm{d}\chi_\mathrm{b}(z)}{\mathrm{d}z}\right] \tag{12b}$$

$$\epsilon_{ssi}(n_i,s_i,z)=-n_i\frac{\mathrm{d}^2\psi_{ni}^{\chi_\mathrm{b}}(s)}{\mathrm{d}s^2}\chi_\mathrm{b}(z) \tag{12c}$$

where the curvilinear coordinate system (n_i,s_i,z) is introduced with $z=R\phi$. We introduced two parameters, ξ_i and ζ_i, defined as

$$\xi_i=\begin{cases}(-1)^{(i-1)/2} & (i=1,3)\\ 0 & (i=2,4)\end{cases} \tag{13}$$

$$\zeta_i=\begin{cases}0 & (i=1,3)\\ (-1)^{(i-2)/2} & (i=2,4)\end{cases} \tag{14}$$

In obtaining the results given in Eq. (12), the following approximation is used as

$$\frac{\partial}{\rho\partial\phi}\approx\left\{1-\xi_i\frac{b}{2R}\right\}\frac{\partial}{\partial z}\quad(i=1,3)$$

$$\frac{\partial}{\rho\partial\phi}\approx\left\{1-\zeta_i\frac{s_i}{R}\right\}\frac{\partial}{\partial z}\quad(i=2,4)$$

The three-dimensional stress components are determined from the constitutive relation as

$$\sigma_{zzi}(n_i,s_i,\phi)=E(\epsilon_{zzi}+v\epsilon_{ssi}) \tag{15a}$$

$$\sigma_{szi}(n_i,s_i,\phi)=2G\epsilon_{szi} \tag{15b}$$

$$\sigma_{ssi}(n_i,s_i,\phi)=E(\epsilon_{ssi}+v\epsilon_{zzi}) \tag{15c}$$

where G is the shear modulus given as $G=E/2(1+v)$.

The system potential energy Π for the present problem can be written as

$$\Pi=\frac{1}{2}\int_{z_1}^{z_2}\int_A\sigma_{kl}\epsilon_{kl}\,\mathrm{d}A\,\mathrm{d}z-\int_{z_1}^{z_2}\int_A(p\tilde{u}_z+q\tilde{u}_s)\,\mathrm{d}A\,\mathrm{d}z-\int_A\left[\bar{\sigma}_{zz}\tilde{u}_z+\bar{\sigma}_{sz}\tilde{u}_s\right]_{z_1}^{z_2}\mathrm{d}A \tag{16}$$

where A is the area of the cross section of the thin-walled curved box beam. The external loads acting in the axial and transverse directions are denoted by p and q. The coordinates z_1 and z_2 $(z_1<z_2)$ represent the locations of two ends of the beam, and $(\bar{})$ denotes the quantities prescribed at the ends.

Substituting Eqs. (12) and (15) into Eq. (16) and integrating the resulting potential energy Π over the beam cross section A yields

$$\begin{aligned}\Pi = \frac{1}{2}\int_{z_1}^{z_2} \Big[& E\Big(e_1 u'^2 + e_2 v^2 + e_3 \beta'^2 + 2e_4 u' v + 2e_5 u'\beta' + 2e_6 v\beta'\Big) \\ & + E\Big(g_1\chi_b^2 + 2g_{11}u'\chi_b + 2g_9 v\chi_b + g_3\chi_b^2 + 2g_7\beta'\chi_b + 2v g_2\chi_b^2\Big) \\ & + G\big(f_1 u^2 + f_2 v'^2 + f_3\beta^2 + 2f_4 uv' + 2f_5 u\beta + 2f_6 v'\beta + h_1\chi_b'^2\big)\Big]\,\mathrm{d}z \\ & - \int_{z_1}^{z_2} (p_1 u + q_1 v + p_2\beta + q_2\chi_b)\mathrm{d}z - \big[\overline{T}u + \overline{V}v + \overline{M}\beta + \overline{X}\chi_b\big]_{z_1}^{z_2}\end{aligned} \tag{17}$$

where $(\ )'$ denotes the differentiation with respect to z. In Eq. (17), the coefficients, such as e, f, g, and h's, can be found by integrating the deformation shape functions. For instance,

$$e_1 = \sum_{i=1}^{4}\int_{A_i}\left\{\xi_i^2\left(1+\xi_i\frac{b}{2R}\right)+\zeta_i^2\left(1+\zeta_i\frac{s}{R}\right)\right\}^2\left(\psi_{\phi i}^u(s_i)\right)^2\mathrm{d}A_i$$

$$f_1 = \sum_{i=1}^{4}\int_{A_i}\frac{\zeta_i^2}{R^2}\left(1+\zeta_i\frac{s}{R}\right)^2\left(\psi_{\phi i}^u(s_i)\right)^2\mathrm{d}A_i$$

The explicit expressions of other coefficients are skipped here.

The definitions of tangential force $\overline{T}$, radial force $\overline{V}$, in-plane bending moment $\overline{M}$, and transverse bimoment $\overline{X}$ prescribed at the ends of a beam are

$$\overline{T} \equiv \sum_{i=1}^{4}\int_{A_i}\sigma_{zzi}\psi_{zi}^u\,\mathrm{d}A_i, \qquad \overline{V} \equiv \sum_{i=1}^{4}\int_{A_i}\sigma_{szi}\psi_{si}^v\,\mathrm{d}A_i$$

$$\overline{M} \equiv \sum_{i=1}^{4}\int_{A_i}\sigma_{zzi}\psi_{zi}^\beta\,\mathrm{d}A_i, \qquad \overline{X} \equiv \sum_{i=1}^{4}\int_{A_i}\sigma_{szi}\psi_{ni}^{\chi_b}\,\mathrm{d}A_i$$

and p_1, q_1, etc. are defined as

$$p_1 = \sum_{i=1}^{4}\int_{A}p\psi_{zi}^u\,\mathrm{d}A_i, \qquad q_1 = \sum_{i=1}^{4}\int_{A}q\psi_{si}^v\,\mathrm{d}A_i$$

$$p_2 = \sum_{i=1}^{4}\int_{A}p\psi_{zi}^\beta\,\mathrm{d}A_i, \qquad q_2 = \sum_{i=1}^{4}\int_{A}q\psi_{ni}^{\chi_b}\,\mathrm{d}A_i$$

Using the principle of the minimum potential energy, we obtain the following one-dimensional governing equations as

$$-E\{e_1u'' + e_4v' + e_5\beta'' + g_{11}\chi_b'\} + G(f_1u + f_4v' + f_5\beta + h_5\chi_b') = p_1$$

$$E\{e_4u' + e_2v + e_6\beta' + g_9\chi_b\} - G(f_4u' + f_2v'' + f_6\beta' + h_4\chi_b'') = q_1$$

$$-E\{e_5u' + e_6v' + e_3\beta'' + g_7\chi_b'\} + G(f_5u + f_6v' + f_3\beta + h_3\chi_b') = p_2$$

$$E\{g_{11}u' + g_9v + g_7\beta' + (g_1 + g_3 + 2vg_2)\chi_b\} - Gh_1\chi_b'' = q_2$$

4. Numerical studies

Since the finite element formulation is well-established, no explicit procedure to determine the stiffness matrix **K** and other quantities needs to be given here. However, the reduced integration scheme (see, e.g., Prathap, 1993) is employed to avoid locking problems. Note that once one-dimensional results are found, the three-dimensional displacement $\tilde{\mathbf{u}}(n,s,\phi)$ and stress $\sigma(n,s,\phi)$ can be obtained using the equations derived in the previous section.

4.1. Case study 1: Applied bending moment at one end

As the first example, we return to the beam under a tip bending moment $M = 1$ Nm, which was considered in Section 2. The present results by the higher-order one-dimensional theory are compared in Fig. 7 with those by the plate finite element and the Timoshenko beam theory. (The number of the present beam elements used in this example is 80.) As is obvious from Fig. 7, the consideration of the additional bending

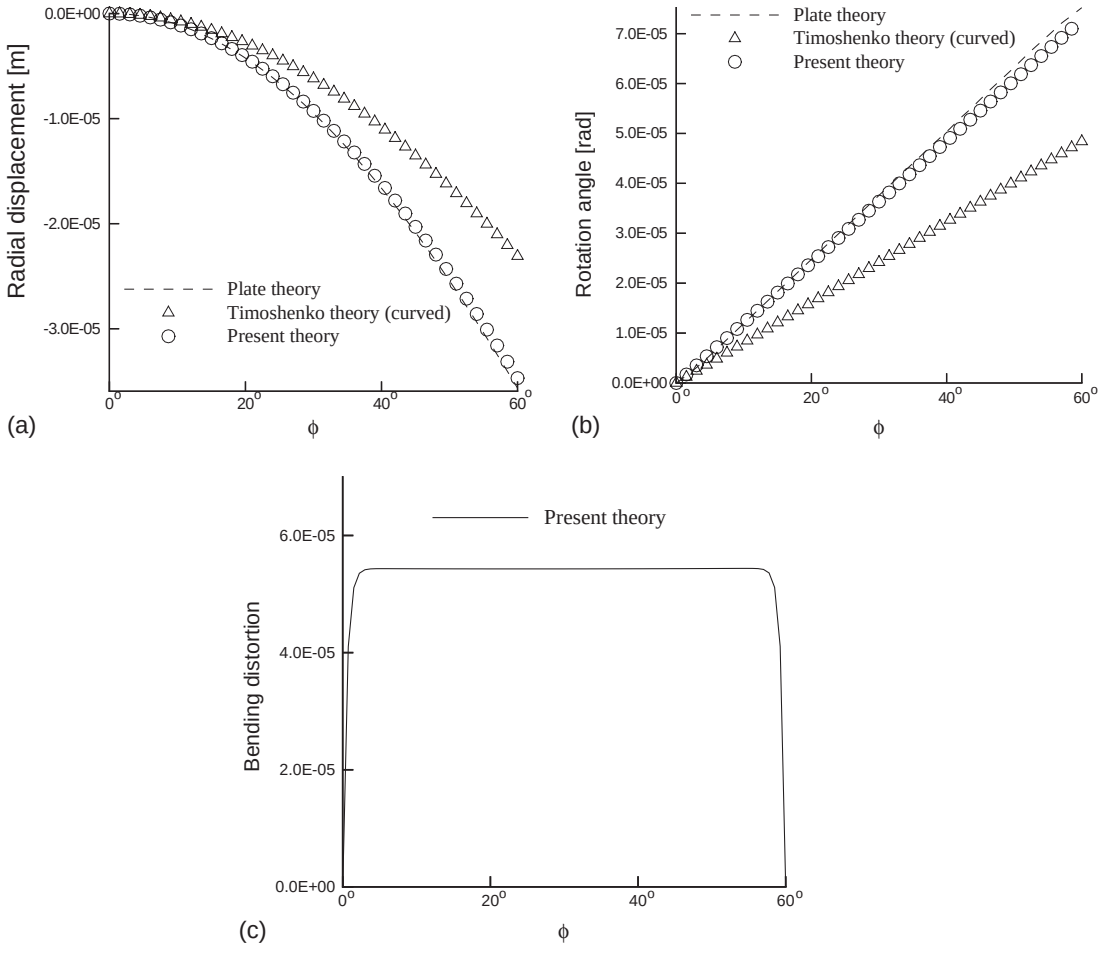

Fig. 7. (a) Radial displacement $v(\phi)$, (b) rotation angle $\beta(\phi)$, and (c) the amount of bending distortion $\chi_b(\phi)$ for the problem depicted in Section 2.

distortional deformation χ_b improves the solution accuracy remarkably. Although the stress field due to the bending distortion is self-equilibrating, its effect on the overall structural flexibility is not negligible in thin-walled curved beams.

4.2. Case study 2: Applied concentrated radial force at one end

We consider a cantilevered thin-walled curved box beam loaded at one end by a radial force $V = 1$ Nm ($T = M = 0$), where the cross section deformation is constrained by a rigid plate. The beam is of width $b = 40$ mm, height $h = 80$ mm, wall thickness $t = 1$ mm, mean radius $R = 0.8$ m, central angle $\Phi = 120°$. The material properties are the same as those for the previous example.

Fig. 8 compares the distribution of the radial displacements along the centerline of the inner wall ($s_1 = 0$ at wall 1), which are obtained by different theories. To determine the radial displacement along the centerline of the inner wall from the present beam theory, the following equation is utilized as (see Eq. (10))

$$v_{(\text{centerline of wall 1})} = -u_{n1}(s_1 = 0, \phi) = -\left(\psi^{u}_{n1}(s_1 = 0)u(\phi) + \psi^{\chi_b}_{n1}(s_1 = 0)\chi_b(\phi)\right)$$

As was in the previous example, the conventional Timoshenko beam theory using three degrees of freedom does not yield satisfactory results.

4.3. Case study 3: Effect of curvature

It is worth investigating how the bending distortion χ_b affects the beam flexibility depending on the mean radius R of the beam curvature. To this end, we consider a cantilevered thin-walled curved box beam loaded by the tangential force $T = 1$ N ($V = M = 0$ in Fig. 2). The beam is of width $b = 25$ mm, height $h = 50$ mm, wall thickness $t = 1$ mm, central angle $\Phi = 90°$, and the material properties are the same as those for the previous examples. The tip displacements of tangential direction is calculated for different values of R, ranging from $R = 0.25$ to 2 m.

The tangential displacements at the tip are predicted by the present beam, the Timoshenko beam and the plate finite element analyses. The tangential displacements plotted in Fig. 9 are relative values divided by the plate finite element results. (The convergence of all the numerical results are checked.) Fig. 9 shows that the contribution of the bending distortion χ_b on the beam flexibility is significant unless the beam curvature

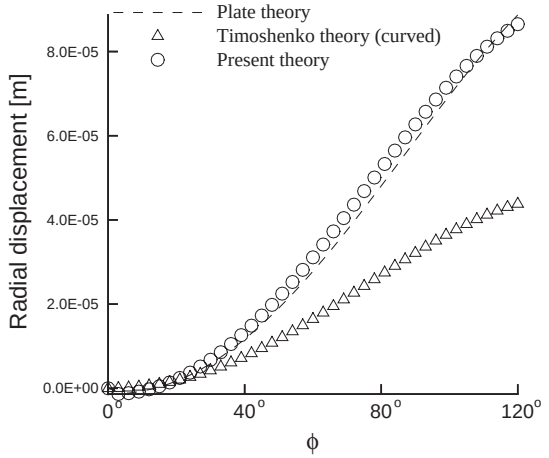

Fig. 8. The radial displacement along the center line of wall 1.

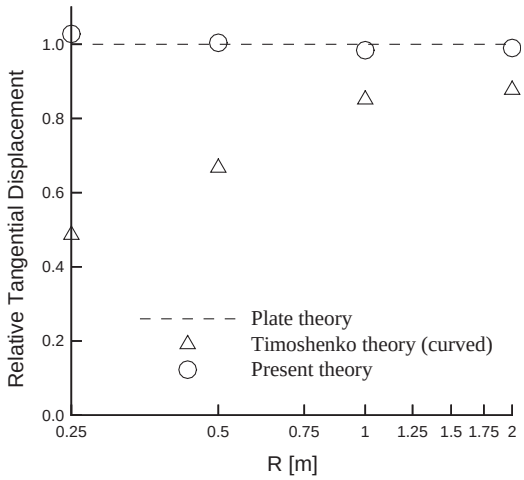

Fig. 9. The effect of the radius of curvature R on the beam flexibility.

is small. The finding from Fig. 9 also justifies the effectiveness of the present higher-order thin-walled curved box beam theory.

5. Conclusion

A higher-order one-dimensional beam theory was developed for the accurate prediction of thin-walled curved box beams under in-plane flexure. For the theory, an approximate in-plane symmetric distortional deformation shape was determined, and the one-dimensional field equations having the three Timoshenko kinematic variables and the additional variable for the in-plane bending distortion were derived. Several case studies confirmed the significant effects of the bending distortional deformations on the bending flexibility in thin-walled *curved* box beams. Furthermore, it was shown that the bending distortion deformation cannot be ignored unless the beam curvature is very small.

References

Beskin, L., 1945. Bending of curved thin tubes. Journal of Applied Mechanics 67A, 1–7.

Dabrowski, R., 1968. Curved Thin-Walled Girders. Cement and Concrete Association, London.

Fu, C.C., Hsu, Y.T., 1995. The development of an improved curvilinear thin-walled Vlasov element. Computers & Structures 54, 147–159.

Hu, Z., Li, J.Q., 1999. Computer simulation of pipe-bending processes with small bending radius using local induction heating. Journal of Materials Processing Technology 91, 75–79.

I-DEAS, 1993. I-DEAS FEM User's Guide. SDRC, Ohio.

Kim, Y.Y., Kim, J.H., 1999a. Thin-walled closed box beam element for static and dynamic analyses. International Journal for Numerical Methods in Engineering 45, 473–490.

Kim, J.H., Kim, Y.Y., 1999b. Analysis of thin-walled closed beams with general quadrilateral cross sections. Journal of Applied Mechanics 66 (4), 904–912.

Kim, J.H., Kim, Y.Y., 2000. One-dimensional analysis of thin-walled closed beams having general cross sections. International Journal for Numerical Methods in Engineering 49, 653–668.

Kim, Y.Y., Kim, Y., 2002. A one-dimensional theory of thin-walled curved rectangular box beams under torsion and out-of-plane bending. International Journal for Numerical Methods in Engineering 53, 1675–1693.

Kim, J.H., Kim, H.S., Kim, D.W., Kim, Y.Y., 2002. New accurate efficient modeling techniques for the vibration analysis of T-joint thin-walled box structures. International Journal of Solids and Structures 39, 2893–2909.

Krístek, V., 1979. Theory of Box Girders. John Wiley & Sons, Chichester.

Lewis, G.D., Chao, Y.J., 1990. Flexibility of trunnion piping elbows. Journal of Pressure Vessel Technology 112, 184–187.

Paulsen, F., Welo, T., 2001. Cross-sectional deformations of rectangular hollow sections in bending: Part II—Analytical models. International Journal of Mechanical Sciences 43, 131–152.

Prathap, G., 1993. The Finite Element Method in Structural Mechanics. Kluwer Academic Publishers, Dordrecht.

Vlasov, V.Z., 1961. Thin Walled Elastic Beams, second ed. The Israel Program for Scientific Translations, Jerusalem.

Whatham, J.F., 1986. Pipe bend analysis by thin shell theory. Journal of Applied Mechanics 53, 173–180.